

Quantitative Measurements of Autofluorescence with the Scanning Laser Ophthalmoscope

Appendix

Optical and Theoretical Considerations

- A. Confocal scanning laser ophthalmoscope (cSLO)**
- B. Quantitative AF: radiometric considerations**
- C. Experimental verification of the square law [Eq. (4)]**
- D. Magnification and scaling factor**
- E. Fundus cameras**
- F. Correction for the absorption by the ocular media**

A. Confocal scanning laser ophthalmoscope (cSLO)

A schematic representation of a SLOs optics (HRA2 and Spectralis HRA-OCT, Heidelberg Eng., Heidelberg, Germany) is given in Fig. A1. Horizontal and vertical optical scanners deflect the laser beam (solid black; solid state laser diode, 488 +/- 2nm) to scan the intermediate plane of the camera and retina in a raster pattern. The laser beam is focused by the optics of the eye to a $\approx 10\mu\text{m}$ spot on the retina. The beam oscillates around a 3mm diameter disk, the so-called scan pupil, conjugated to the plane of the scan mirrors. The scan pupil needs to be aligned in all three dimensions onto the subject's anatomical pupil (iris).

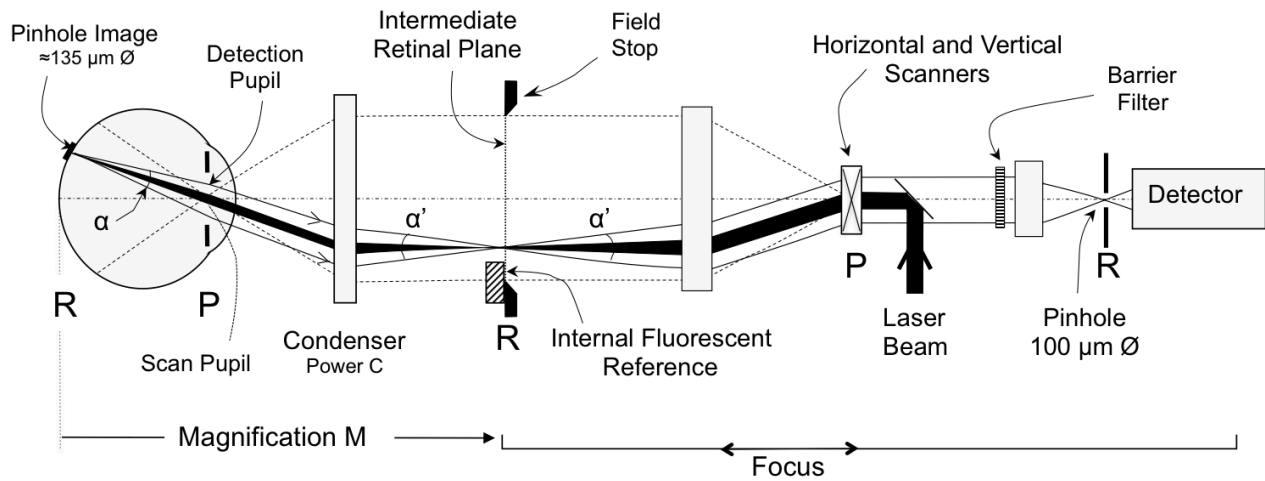


Figure A1. Schematic diagram of a confocal Scanning Laser Ophthalmoscope. Conjugated retinal and pupil planes are indicated by R and P, respectively. Focus of the retinal image is achieved by translating the intermediate plane and all optical and electronic components to its right (bracket).

The detection pupil of the optical system captures the reflected and fluorescent light (solid lines) that originates from the retinal spot (cone with full angle α). The detection pupil is a 6-mm diameter area (concentric to the scan pupil) that is conjugated to the scan mirrors. The detected light is first imaged in the intermediate plane and then inside the pinhole (several optical elements were omitted). The pinhole in front of the detector, when imaged onto the retina, covers an area much larger than the $\approx 10\mu\text{m}$ -diameter laser spot. The pinhole image is significantly larger than the laser spot on the retina. Therefore the capture of the fluorescence is completely defined by the size of the detection pupil.

The internal fluorescence reference is mounted on the field stop so that its fluorescent surface is facing the laser beam. The AF from the reference is captured by a cone with full angle α' . The field stop defines a square area limiting the image to the 30°x30° field. Smaller fields are obtained by limiting the amplitude of the vertical slow scanner, and by omitting the outer pixels of the horizontal scan line with unchanged horizontal scan amplitude. Thus, only the vertical extension of fundus illumination is reduced to alter field size, whereas its horizontal extent remains unchanged at 30°. The internal reference is therefore only usable with the 30° field.

B. Quantitative AF: radiometric considerations

Fluorescence emitted from the RPE is assumed to have an isotropic (angular) distribution at least in the solid angle (3-dimensional angle) directed towards the pupil of the eye. This distribution will not be substantially altered by passage through the cones.¹ We also assume that the distribution will be minimally affected by directional effects in the rods and by light scattering in the blood vessels and the nerve fiber layer.

Fluorescence emitted from one retinal position upon excitation by the laser beam with radiant power P_B (Watts) is thus emitted in all directions, with almost instantaneous radiant intensity $\xi_F \times P_B$ (Watt/sr; the steradian – sr - is the unit of “solid angles”). The efficacy ξ_F of the fundus fluorophores depends upon the absorption of the excitation light, and on the quantity and quantum efficiency of the fluorophores (the latter could vary with changes in the chemical environment without a change in the amount of pigment). The fraction of the emitted light that is comprised within the solid angle $(\pi/4) \times \alpha^2$ will reach the pinhole and thus the detector (Fig. A1). The instantaneous radiant power through the pinhole is then:

$$P_F = \xi_F \times P_B \times \frac{\pi}{4} \times \alpha^2 \times \overline{T}_\Lambda \times \overline{T}_\lambda \quad (1)$$

\overline{T}_Λ and \overline{T}_λ are the transmissions through the ocular media of the excitation light and emitted fluorescence, respectively (wavelengths Λ and λ , respectively). The bar notation indicates that these transmissions are calculated by averaging to account for the spectral characteristics of the fundus AF, the detector, and the excitation light

(fundus camera). For the internal reference, with a fluorescence efficiency ξ_R , the power detected by the pinhole is:

$$P_R = \xi_R \times P_B \times \frac{\pi}{4} \times \alpha^2 \quad (2)$$

The solid angle $(\pi/4) \times \alpha^2$ is fixed and defined by the optics (Fig. A1).

The signal output of the detector is linearly amplified and partitioned both in intensity (255 gray levels or GL) and in space ($N \times N$ pixels).² The GLs corresponding to the amplified signal P_F and P_R are GL_F and GL_R , respectively. The dark-signal level is digitized as GL_0 . Thus, $GL_F - GL_0$ is proportional to the light power reaching the detector and to the gain G of the detector and other amplifiers. To eliminate the power P_B and gain G , we calculate the ratio:

$$\frac{GL_F - GL_0}{GL_R - GL_0} = \frac{G \times P_F}{G \times P_R} = \frac{\xi_F}{\xi_R} \times \left(\frac{\alpha}{\alpha'} \right)^2 \times \overline{T_\Lambda} \times \overline{T_\lambda} \quad (3)$$

after substitution of P_F and P_R from Eq. (1) and (2), respectively. The Smith-Helmholtz formula³ states that $M \times \alpha' = n \times \alpha$, where n is the refractive index of the vitreous and M is the magnification between the retina and the intermediate plane. The efficacy of the fundus fluorophore can then be derived from Eq. (3) as:

$$\xi_F = \frac{GL_F - GL_0}{GL_R - GL_0} \times n^2 \times \xi_R \times \frac{1}{M^2} \times \frac{1}{\overline{T_\Lambda} \times \overline{T_\lambda}} \quad (4)$$

Practically, we rename ξ_F as quantified AF (qAF), and perform the following transformation to normalize both M and $\overline{T_\Lambda} \times \overline{T_\lambda}$:

$$qAF = \left[\frac{n^2 \times \xi_R}{M_{em,7.7}^2 \times \overline{T_{\Lambda,20}} \times \overline{T_{\lambda,20}}} \right] \times \frac{GL_F - GL_0}{GL_R - GL_0} \times \left(\frac{M_{em,7.7}}{M} \right)^2 \times \frac{\overline{T_{\Lambda,20}} \times \overline{T_{\lambda,20}}}{\overline{T_\Lambda} \times \overline{T_\lambda}} \quad (5)$$

$M_{em,7.7}$ is the magnification M for an emmetropic eye with average corneal curvature of 7.7mm, and $\overline{T_{\Lambda,20}} \times \overline{T_{\lambda,20}}$ are the media transmissions of an average 20year-old subject.

These normalizations minimize errors in estimating these factors. The term in the square parenthesis is the “reference calibration factor (RCF)”. It depends upon the fluorescent material used for the reference, the cSLO type (or fundus camera) used ($M_{em,7.7}$), and the normalization of the media transmission. RCF was not calculated as such. Instead, RCF is defined directly by calibration of the system (with its internal

reference in place) with a Master Reference, and its value adjusted by a constant so that the average qAF for a group of 20-year-old subjects be 200qAF-units (the exact protocol to achieve this is under development). Thus, Eq. (5) becomes:

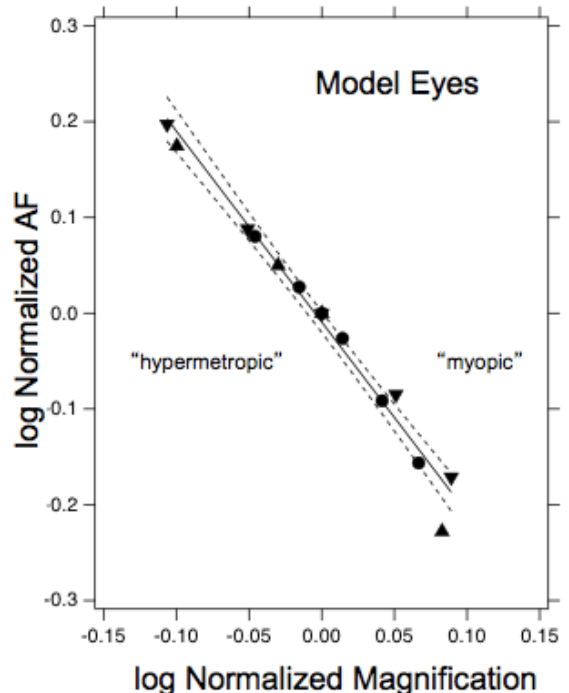
$$qAF = RCF \times \frac{GL_F - GL_0}{GL_R - GL_0} \times \left(\frac{M_{em,7.7}}{M} \right)^2 \times \frac{\overline{T_{\Lambda,20}} \times \overline{T_{\lambda,20}}}{\overline{T_{\Lambda}} \times \overline{T_{\lambda}}} \quad (6)$$

Thus, qAF represents the autofluorescence of the fundus relative to that which would be measured through the media of a 20-year-old emmetropic eye with average dimensions.

C. Experimental verification of the square law [Eq. (4)]

To investigate the dependence of the recorded AF on the magnification M from the retina to the intermediate plane (Eq. 4), we recorded images from model eyes incorporating fluorescent “retinal” targets to simulate AF imaging. The “axial length” was varied over a wide range. The magnifications were determined from the distances between fixed points on the image of the targets. Average GL were measured in a small area in the middle of the field, and corrected for changes in the sensitivity and zero GL. The AF decreased with the square power of the magnification from the target “retina” to the intermediate plane (Fig. A2).

Figure A2. Variation of AF with magnification from the “retinal” target in the model eyes to the intermediate image plane of the camera, for the case simulating fundus AF (filled symbols). Both AF and magnification were normalized to their respective values at the emmetropic position of the targets. The different symbols are for different model eyes. The linear fit to the data for the simulated case yielded a slope of -1.97 (S.E.=0.09; $r^2=0.97$; $p<0.0001$).



D. Magnification and scaling factor

Magnification. To calculate the magnification, M , between the retina and the intermediate plane (needed in Eq. 6) we use the Gullstrand-Emsley model⁴ under the assumption that the optical power of the crystalline lens and its axial position are constant and equal to those given by the Gullstrand-Emsley model. In addition, measurement of either the corneal curvature (by keratometry) or the axial length of the eye (by A-scan ultrasound biometry or Optical Coherence Tomography) is required.

We use the same notations as in most of the literature on this subject.⁴⁻⁶ The magnification M from the retina to the intermediate plane is given by:

$$M = \frac{f_{condenser}}{k'/n_4} = \frac{F_0 + K}{C} \quad (7)$$

where $f_{condenser}$ and C are the focal length (mm) and optical power of the condenser lens of the camera, k' the distance from the 2nd principal plane of the eye to the retina, n_4 the refractive index of the vitreous ($n_4=1.333$), F_0 is the power of the eye (diopters), and K the refractive error (diopters). The power of the condenser lens of the camera is $C=32.36$ diopters, for both the HRA2 and the Spectralis. The power of the eye is:

$$F_0 = F_1 + F_L - \frac{d \times F_1 \times F_L}{1000 \times n_2} \quad (8)$$

where F_L is the power of the crystalline lens ($F_L=21.76$ diopters), d is the distance between the corneal apex and the 1st principal plane of the crystalline lens ($d=5.747$ mm), 1000 mm/m is the conversion factor (d in mm; $1D=1m^{-1}$), n_2 the refractive index of the aqueous humor ($n_2=1.333$), and F_1 is the power of the anterior surface of the cornea. The later is given by:

$$F_1 = \frac{1000 \times (n_2 - 1)}{r_1} \quad (9)$$

Assuming that F_L , d , n_2 and n_4 are constant among individuals, as stated above. If the radius of curvature r_1 of the cornea is known (measured), then M is computed by successive substitutions using Eqs. (7-9).

The axial length of the eye (in mm), AxL , is the sum of the distance of the corneal apex to the 2nd principal plane of the eye ($A1P'$) and the distance k' of that principal plane to the retina. Thus, F_0+K can be expressed as:

$$F_0 + K = \frac{1000 \times n_4}{AxL - A1P'} \quad (10)$$

The position of the 1st principal plane, $A1P'$, is affected by all optical parameters of the model eye, but the individual variations in $A1P'$ are small and have a relatively small effect on F_0+K . We therefore use the “adjusted axial length method” described by Bennett et al⁴ in which $A1P'$ is fixed at 1.83mm (Gullstrand-Emsley model; $r_1=7.7$ mm). If the axial length is known (measured), then M is computed by substitution of F_0+K in Eq. (7).

Scaling Factor. The magnification can also be expressed as a “scaling factor” (SF) that gives the retinal dimension (in μm) corresponding to 1 pixel in the image. If d_{IP} x d_{IP} is the dimension of the square image in the intermediate plane ($d_{IP}=16.65\text{mm}$), then the size of 1 pixel in that plane is d_{IP}/N , where N is the number of pixels along the side of the image (768 or 1536, for “high speed” or “high resolution”, respectively). The magnification from the intermediate plane to the retina is $1/M$, with M given by Eq. (7). Therefore, the scaling factor (in $\mu\text{m}/\text{pixel}$) can be equated as:

$$SF = 1000 \times \frac{d_{IP}}{N} \times \frac{C}{F_0 + K} \quad (11)$$

The factor 1000 $\mu\text{m}/\text{mm}$ accounts for d_{IP} being expressed in mm and SF in $\mu\text{m}/\text{pixel}$. Variation of SF with r_1 and K or with AxL is shown in Fig. A3 (next page).

The HRA2 and Spectralis system software provides (in the “image info”) SFs that were computed by ray tracing using a model eye that incorporated a gradient index crystalline lens (Dr. G. Zinser, personal communication, 2010). In Fig. A3 we compare SF obtained from the software with those calculated from the Gullstrand-Emsley eye model using Eq. (11).

To avoid confusion, we suggest using the reference corneal curvature of 7.7mm (default software value), instead of 7.86mm for the Gullstrand-Emsley model eye. Eqs. (7) to (11) can be used to calculate SF in special situations and for animal studies, given that the optical parameters are known.

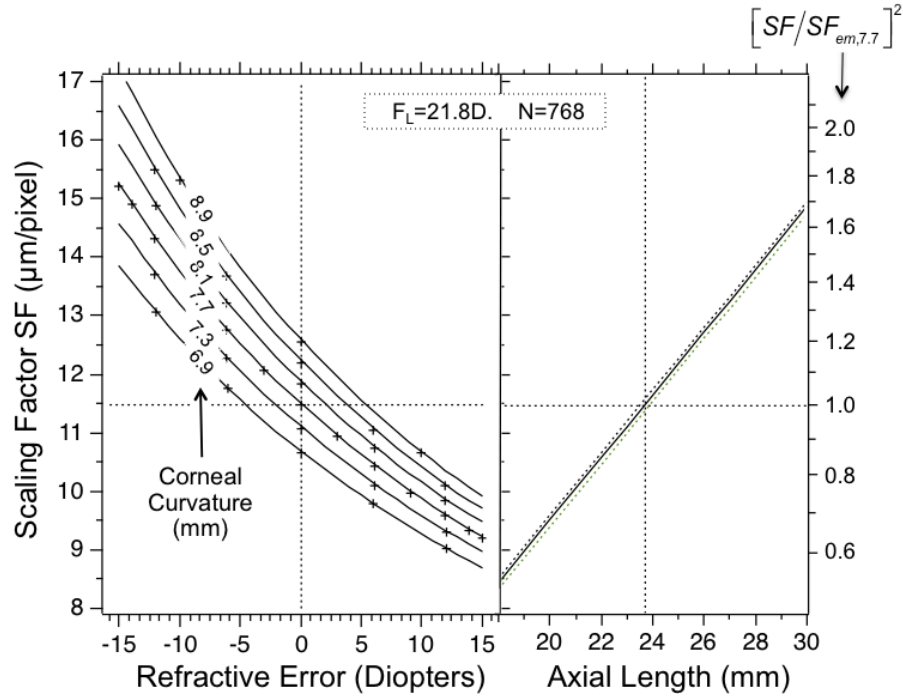


Figure A3. Left: Scaling factor, SF , as a function of refractive error and corneal curvatures, derived from the Gullstrand-Emsley model eye (lines) using Eqs. (7), (8), (9) and (11) is compared with SF from the system software (crosses); the largest difference between to 2 estimates of SF is 0.4%. Right: Scaling factor, SF , as a function of axial length (sloped line) derived from Eqs. (10) and (11). The 2 sloped interrupted lines were calculated for the extreme corneal curvatures (6.9 and 8.9 mm); it demonstrates that changes in corneal curvature have little effect on M and SF . The scale on the right displays the actual correction factor $[SF/SF_{em,7.7}]^2$ as used in Eq. (12), where $SF_{em,7.7}=11.5 \mu\text{m/pixel}$ (SF for an emmetropic eye with a corneal curvature of 7.7mm).

Substitution of SF from Eq. (11) into Eq. (6) gives the practical form used to derive the quantified autofluorescence qAF :

$$qAF = RCF \times \frac{GL_F - GL_0}{GL_R - GL_0} \times \left(\frac{SF}{SF_{em,7.7}} \right)^2 \times \frac{\overline{T_{\lambda,20}} \times \overline{T_{\lambda,20}}}{\overline{T_{\lambda}} \times \overline{T_{\lambda}}} \quad (12)$$

Note that the correction factor $(SF / SF_{em,7.7})^2$ is independent of the parameters C , d_{IP} , and N .

E. Fundus cameras

An internal reference could also be incorporated into a fundus camera. The intermediate plane in all fundus cameras is located behind the condenser (it is the plane in which the fixation stick is moved), and at a fixed distance from the first lens in the detection optics. Thus, the internal reference must be mounted on a mechanical extension that is fixed to the housing of that first lens, so that it is always in the intermediate plane. In fact, a similar situation exists in the older HRAC (Heidelberg Eng., Heidelberg, Germany). Radiometric considerations for quantifying AF with a non-confocal system lead to a relationship similar to Eq. (4); the quasi-uniform retinal irradiance varies with $1/M^2$ and the light collected by the detection system is independent of refractive state (conservation of optical extend).^{2, 7}

F. Correction for the absorption by the ocular media

Individual correction for the losses caused by the absorption by the ocular media will be achieved by a reflectometry technique (under development). However, in some studies (e.g. a comparison of groups of young and old subjects) it may be sufficient to employ an algorithm that predicts the average media optical density for a given age and wavelength.^{8, 9} The algorithm of van de Kraats and van Norren,⁹ is based on 6 optical density components, of which only 3 play a significant role if wavelengths are restricted to the 480-740nm range. The optical density $D_{\lambda, \text{Age}}$, at a wavelength λ and *Age*, is given by the algorithm:

$$D_{\lambda, \text{Age}} = 1.43 \times \left[0.016 + 1.32 \times 10^{-4} \times \text{Age}^2 \right] \times \exp \left\{ - \left(\frac{\lambda - 325}{125} \right)^2 \right\} + \left[R + 3.1 \times 10^{-4} \times \text{Age}^2 \right] \times \left\{ \frac{400}{\lambda} \right\}^4 + 0.111 \quad (13)$$

The first term is associated with the aging lens based on donor lens measurements from Ambach et al.¹⁰ The second term is Rayleigh light scattering, with *R* being a field-size dependent constant (*R*=0.45 for the 1°-diameter retinal field, and *R*=0.22 for fields >3°). The value for *R* may be much larger for the field covered by the scanning laser

beam. The last term (0.111) is a wavelength and age neutral term that presumably accounts for large particle scattering in the lens and vitreous.⁹ By referencing the media transmission to that of a 20year-old subject, we effectively eliminate from Eq. (13) the R and 0.111, the 2 terms that exhibit large uncertainties. We used an excitation wavelength of $\Lambda=485.5\text{nm}$ (mid-range of the laser diodes' peak wavelengths) and a mean emission wavelength of $\lambda=637\text{nm}$ (average wavelength of the fundus emission spectrum over the media transmission spectrum, $10^{-D\lambda}$). We found, after multiple uses of Eq. (13), that the media transmission term of Eq. (12) can be expressed as:

$$\frac{\overline{T_{\Lambda,20}} \times \overline{T_{\lambda,20}}}{\overline{T_{\Lambda}} \times \overline{T_{\lambda}}} = 10^{5.56 \times 10^{-5} \times (\text{Age}^2 - 400)} \quad (14)$$

The simple relationship can be used to calculate the magnitude of the media losses. Note that the often-used algorithm of Pokorny et al.⁸ gives similar results as Eq. (14) up to age 60years, but appears to overestimate densities for older subjects,¹¹ probably due to inclusion of eyes with cataracts in the initial studies (Dr. J. Pokorny, personal communication, 2010).

References

1. Prieto PM, McLellan JS, Burns SA. Investigating the light absorption in a single pass through the photoreceptor layer by means of the lipofuscin fluorescence. *Vision Research* 2005;45:1957-1965.
2. Webb RH, Dorey CK. The pixilated image. In: Pawley JB (ed), *Handbook of Biological Confocal Microscopy*. New York: Plenum Press; 1995:55-67.
3. Born M, Wolf E. *Principles of Optics*. NY: The Macmillan Company; 1964.
4. Bennett AG, Rabbetts RB. *Clinical Visual Optics*: London. Butterworths; 1984.
5. Bennett AG, Rudnicka AR, Edgar DF. Improvements on Littmann's method of determining the size of retinal features by fundus photography. *Graefe's Arch Clin Exp Ophthalmol* 1994;232:361-367.
6. Rudnicka AR, Burk ROW, Edgar DF, Fitzke FW. Magnification characteristics of fundus imaging systems. *Ophthalmology* 1998;105:2186-2192.
7. Delori FC. Spectrophotometer for noninvasive measurement of intrinsic fluorescence and reflectance of the ocular fundus. *Applied Optics* 1994;33:7439-7452.
8. Pokorny J, Smith VC, Lutze M. Aging of the human lens. *Appl Opt* 1987;26:1437-1440.
9. van de Kraats J, van Norren D. Optical density of the young and aging human ocular media in the visible and the UV. *JOSA A* 2007;24:1842-1857.
10. Ambach W, Blumthaler M, Schoft T, et al. Spectral transmission of the optical media of the human eye with respect to keratitis and cataract formation. *Doc Ophthalmol* 1994;88:165-173.
11. Moreland JD, Torczynski E, Tripath R. Rayleigh and Moreland matches in the aging eye. *Doc Ophthalmol Proc Ser* 1991;54:347-352.